CFD Letters

Journal homepage:
https://semarakilmu.com.my/journals/index.php/CFD_Letters/index
ISSN: 2180-1363

Simulation Approach of Photovoltaic Thermal Based on Water Collector with Rectangular Model

Muhammad Zohri[1,2], Prabowo[1,*], Suwarno[1], Ahmad Fudholi[3,4], Sena Abraham Irsyad[3], Ajeng Tri Rahayu[3], Yadi Radiansah[3], Dalmasius Ganjar Subagio[3], Yusuf Suryo Utomo[3], Aep Saepudin[3]

[1] Department of Mechanical Engineering, Institut Teknologi Sepuluh Nopember (ITS), Surabaya 60111, Indonesia
[2] Department of Physics Education, Universitas Islam Negeri Mataram, Mataram 83116, Indonesia
[3] Center for Energy Conversion and Conservation, National Research and Innovation Agency (BRIN), Jakarta 10340, Indonesia
[4] Solar Energy Research Institute, Universiti Kebangsaan Malaysia, Bangi 43600, Selangor, Malaysia

ARTICLE INFO

Article history:
Received 14 October 2023
Received in revised form 15 November 2023
Accepted 12 December 2023
Available online 31 March 2024

Keywords:
Photovoltaic Thermal; Collector; Rectangular; Efficiency; Thermal

ABSTRACT

The advancement of PVT technology in the contemporary era is experiencing an upward trend. This phenomenon can be attributed to the growing societal demand for energy, particularly renewable energy derived from solar sources. The present study investigates the rectangular configuration of a water-based heat absorber within a photovoltaic-thermal (PVT) system. The rectangular model PVT system was simulated using nine different mass flow rate of water variations within the rectangular model channel. The dataset has nine mass flow rate of water variants ranging from 0.001 kg/s to 0.009 kg/s, as well as six solar radiation variations: 500 W/m^2, 600 W/m^2, 700 W/m^2, 800 W/m^2, 900 W/m^2, and 1000 W/m^2. The maximum average outlet temperature achieved under 1000 W/m^2 solar radiation is 50.53%, given a 0.001 kg/s fluid mass flow rate. The maximum average photovoltaic (PV) efficiency is 11.93% when exposed to 500 W/m^2 solar radiation intensity. The maximum average photovoltaic-thermal (PVT) efficiency is 76.23% when exposed to 500 W/m^2 solar radiation intensity. Therefore, utilizing rectangular collectors in water-based photovoltaic-thermal systems potentially substantially enhanced the average thermal efficiency and overall PVT efficiency. Consequently, it is advisable to consider incorporating rectangular collectors in the future improvements of PVT technology.

1. Introduction

The emergence of renewable and eco-friendly energy technologies presents a promising remedy for tackling environmental issues. New and sustainable energy sources offer many benefits, such as abundant sources, accessibility to everyone, and reliability, particularly solar energy [1]. Solar panels are used to convert solar energy into electricity. However, one drawback of solar panels lies in their relatively low efficiency [2]. Solar panels, also known as photovoltaic technology, transform solar radiation into electrical energy. As radiation levels increase, the temperature of the solar panel also

* *Corresponding author.*
E-mail address: prabowo@me.its.ac.id (Prabowo)

https://doi.org/10.37934/cfdl.16.8.121137

increases. This temperature increase adversely affects the solar panels' performance, resulting in a decline in their overall efficiency [3].

Integrating solar technology and collector technology to capture heat and electricity simultaneously is commonly referred to as photovoltaic thermal (PVT) systems. This emerging technology is widely used in various applications, depending on collectors' specific requirements and utilization. The primary objective of this PVT technology is to efficiently capture and utilize excess thermal energy generated by solar panels while concurrently implementing cooling measures to prevent overheating. PVT technology has found its application in various areas such as food drying, space heating, air conditioning, and providing warm water for residential homes and pools [4]. The efficiency of PVT electrical energy is superior to that of solar panels. Moreover, installing PVT technology offers space and cost savings advantages compared to separately installing collectors and PV systems [5].

Omri *et al.,* [6] have conducted calculations on applying numerical methods to PVT systems incorporating porous deflectors. Adding five porous deflectors to the PVT collector resulted in a temperature decrease of up to 13.7 K. Salman *et al.,* [7] utilized a computational fluid dynamics (CFD) approach to model the duct collector in the PVT system. The computational fluid dynamics (CFD) analysis reveals that the solar panel experiences a temperature decrease to 14 K. Masalha *et al.,* [8] conducted experimental testing and numerical simulations to evaluate the performance of solar panels equipped with porous duct collectors. The findings from simulations and experiments demonstrated a reduction in photovoltaic (PV) temperature by approximately 35.7% and an increase in power output of up to 9.4%.

Khelifa *et al.,* [3] conducted a simulation study on the glass-coated PVT using a CFD approach. Using glass material, the study exhibited an average gain of thermal efficiency of 38%, whereas without glass, the thermal efficiency was measured at 24%. The thermal and electrical efficiency, with and without the presence of glass, was approximately 11.8% and 10.3%, respectively [9]. On a related note, Rosli *et al.,* [10] focused on designing water-based collectors Rosli *et al.,* [10] designed water-based collectors for PVT, incorporating different variations of waterways. The channel models employed consist of square and round tube configurations. Among the four designs that were compared, the square-tube model demonstrated the highest thermal efficiency, reaching 49%. The range of solar radiation utilized ranged from 300 W/m^2 to 1000 W/m^2.

The utilization of crystalline silicon cells in thermal photovoltaic systems has been developed to incorporate natural circulation in an outdoor setting. The achieved daily PVT efficiency results range from 52% to 65% [11]. The impact of sun radiation on the electrical efficiency of Photovoltaic systems is significant. The temperature played a crucial role in both the electrical efficiency and overall performance of solar panels, as stated in a previous study [12]. Various experimental approaches have been employed to investigate solar radiation's impact on solar panels' efficiency and functionality [13]. Variations in collector parameters and configuration in the PVT systems can impact the PV performance due to their influence on heat transfer. Direct-flow collectors are efficient in heat transfer and can be easily modeled [14]. Simulation techniques have been utilized to accurately replicate natural fluid flow in collector models, employing a Computational Fluid Dynamics (CFD) approach [15]. Simulation and modeling approaches have yielded cost-effective outcomes [16]. The optimal electrical efficiency is achieved with a flow rate variation of 0.03 kg/s of SiO2 fluid under 1000 W/m^2 solar intensity.

Rosli *et al.,* [17] have demonstrated through modeling that the electrical efficiency in PVT can be enhanced by increasing the fluid flow rate. The simulation results revealed that the highest electrical efficiency achieved was 11.67%, representing the highest value observed. The high electrical efficiency is attained under specific conditions of a 1000 W/m^2 solar intensity and a 0.005 kg/s flow

rate. Hernando *et al.,* [18] have developed collectors for PVT systems in both round and square models. The simulation findings indicate that various forms or designs of collectors can influence the PVT's overall performance. The implementation of a channel doubling model has the potential to impact both thermal and electrical performance. The electric and thermal performance is reported to be 1.5% and 2.3% respectively [19].

The CFD approach can be used to gain knowledge and comprehension of fluid dynamics, heat transfer, fluid movement, melting process, freezing process, and related phenomena. The CFD approach utilizes numerical techniques to analyze equations, enabling the validation, optimization, design, and resolution of various problems [20]. One of the key advantages of CFD is its ability to model a wide range of boundary conditions and physical circumstances that are impractical to replicate in experimental approaches [21]. In this particular study, a CFD approach is employed to analyze the performance and temperature distribution within a rectangular model channel of a water-based PVT system. As the first objective, this research examines the impact of the PVT rectangular channel on various factors, including outlet temperature, fluid mass flow rate, and temperature distribution of solar panels. Second, it seeks to examine the temperature distribution on the rectangular channel, solar panel temperature, electrical efficiency, thermal efficiency, and overall PVT efficiency. Lastly, the third objective of this study is to investigate the impact of changes in fluid flow rate and solar radiation on the overall performance of the PVT system.

2. Methodology

2.1 Collector Design

This research employed a rectangular channel model to replicate a PVT system used for water drainage. The PVT system comprises solar panels and cooling collector models. Water was commonly employed as a heat transfer medium to cool solar panels. Figure 1 illustrates the arrangement of the solar panel positioned above and the cooling collector placed below. In the simulation, the PVT location is maintained at a constant slope or upright position toward the surface of the solar panel. As depicted in Figure 2, the rectangular model collector channel has a 9445 mm length, a 15 mm channel height, and a 30 mm channel width. These dimensions are specifically designed to facilitate the cooling process of solar panels. The composition of the solar panel material includes several components, such as glass parts, PV cell parts, EVA parts, and Tedlar parts, as detailed in Table 1 [22,23].

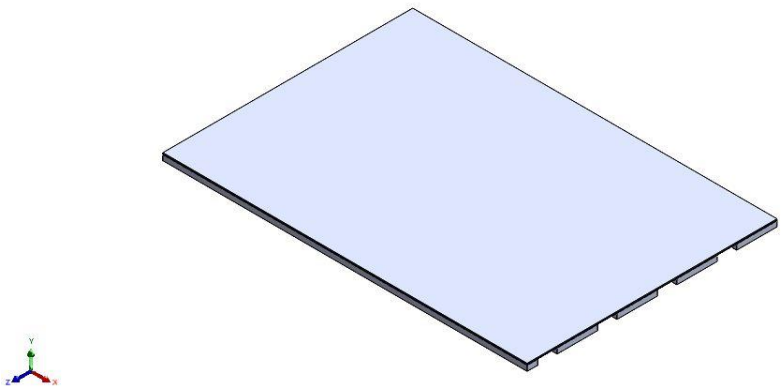

Fig. 1. The solar panel is positioned on top, and the rectangular collector model on the bottom

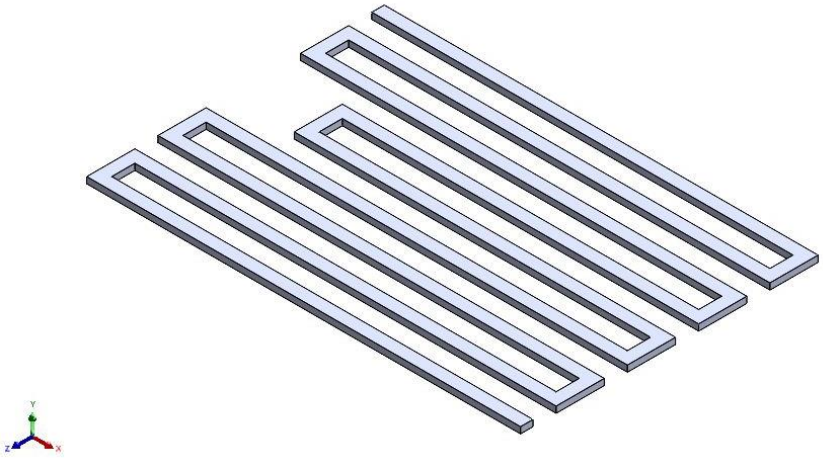

Fig. 2. The water-based rectangular collector channel model on the PVT system

Table 1
Properties of PVT system-based water

Component	Material	Density (Kg/m^3)	Specific heat capacity (J/kg.K)	Thermal conductivity (W/m.K)
PV panel	EVA	2329	700	148
Backsheet	Tedlar	1200	1250	0.15
Rectangular channel	Aluminum	2700	900	160
Fluid	Water	998.2	4182	0.6

The PVT system serves a dual purpose of generating electricity and utilizing solar panel heat to provide simultaneous cooling and heating of water for residential use. This study assumes the PVT model under the specified conditions. First, the flow of water fluid can be either smooth or unobstructed [24]. Second, the condition can be described as either a steady state or an ideal state. Third, the flow rate exhibits characteristics of both transitional and turbulence [25]. Fourth, the combined impact of convective and radiative heat loss is considered [26]. The water fluid flow collector is in direct contact with the solar panel, ensuring the initial temperature is similar [27].

The simulation employed ANSYS Fluent software to examine the water fluid collector PVT. The adjustment of water fluid flow type is conditioned upon using the Reynolds number [28]. The mass flow rate employed is 9, explicitly ranging from 0.001 kg/s to 0.009 kg/s with a 0.001 kg/s increment. The sun intensities used in this study consist of six levels, specifically 500 W/m^2, 600 W/m^2, 700 W/m^2, 800 W/m^2, 900 W/m^2, and 1000 W/m^2. These six solar radiations are projected to encompass low, medium, and high circumstances.

For the Reynold number, the following Eq. (1) explains it.

$$R_e = \frac{\rho V D}{\mu} \tag{1}$$

Where *Re* is the Reynold number, ρ is the density of water, μ is the Dynamic viscosity of water, and D is the hydraulic diameter.

The utilization of k and ε models in this simulation is motivated by the presence of turbulent and transitional flows [29], as seen in the following Eq. (2)-(3). The inlet temperature of the water entering the rectangular collector channel is 25 ºC [30].

For the turbulent kinetic energy (*k*), the equation is

$$\frac{\partial}{\partial t}(\rho k)\frac{\partial}{\partial x_i}(\rho k u_i) = \frac{\partial}{\partial x_j}\left[\left(\mu + \frac{\mu_t}{\sigma_k}\right)\frac{\partial k}{\partial x_j}\right] + P_k - \rho\varepsilon \quad (2)$$

and for the energy dissipation rate equation (ε), the equation is

$$\frac{\partial}{\partial t}(\rho \varepsilon)\frac{\partial}{\partial x_i}(\rho \varepsilon u_i) = \frac{\partial}{\partial x_j}\left[\left(\mu + \frac{\mu_t}{\sigma_\varepsilon}\right)\frac{\partial \varepsilon}{\partial x_j}\right] + C_{1\varepsilon}\frac{\varepsilon}{k}P_k + C_{2\varepsilon}^{*}\frac{\varepsilon^2}{k}\rho \quad (3)$$

2.2 Meshing Strategy

Meshing refers to the process of dividing the geometry into smaller elements and nodes. The meshing process aims to achieve an even distribution of geometry. As the size of an element decreases, the total nodes and elements formed increases. Increasing the amount of elements will enhance the results' accuracy but will also lead to a longer processing time. In contrast, a smaller total element leads to decreased results' accuracy or neatness [31]. This simulation's focal point of meshing is situated on the rectangular collector and solar panel. The quantity of meshing nodes is determined to be approximately 147K**.** Once numerical calculations have been conducted, obtaining a temperature contour diagram is possible. Once an appropriate temperature measurement has been acquired, it becomes possible to calculate and review the distribution of temperature points. The thermal and PV efficiency can be calculated by determining the average temperature of the outlet and PV surface.

2.3 *Governing Equation*

The following equation calculates thermal energy efficiency [32]

$$\eta_{thermal} = \frac{Q_u}{GA_{collector}} \quad (4)$$

Where *G* is solar intensity, $A_{collector}$ is PVT collector area and Q_u is the useful heat gain. For the Q_u, the equation is as follows [33]

$$Q_u = \dot{m}C_p(T_{out} - T_{in}) \quad (5)$$

Where, $\dot{m}$ is the water mass flow, C_p is the water heat capacity, T_{out} is the fluid output temperature during simulation, T_{in} is the fluid input temperature during simulation [34,35].

The PVT system's electrical efficiency is calculated by the following equation [36]

$$\eta_{elec} = \frac{P_{maximum}}{GA_{collector}} \quad (6)$$

$$P_{maximum} = I_{max}V_{max} = FFI_{sc}V_{oc} = \eta_{cell}A_{cells}\alpha_{pv}G \quad (7)$$

$$\eta_{cell} = \eta_{ref}\left(1 - \beta_{ref}\left(T_{out} - T_{ref}\right)\right) \quad (8)$$

For the total efficiency of the PVT system, the following equation can calculate the result [37]

$$\eta_{total\_PVT} = \eta_{cell} + \eta_{thermal} \quad (9)$$

3. Results

The present study used a simulation methodology to investigate the performance of a rectangular collector model in a PVT system, utilizing water as the working fluid. The dataset consists of nine distinct measurements of fluid mass flow rates. The average fluid mass flow rate ranges from 0.001 kg/s to 0.009 kg/s, with an increment of 0.001 kg/s. The intensity of solar radiation exhibits six distinct changes. The six measured intensities of solar radiation are 500 W/m^2, 600 W/m^2, 700 W/m^2, 800 W/m^2, 900 W/m^2, and 1000 W/m^2. It is anticipated that the variations in water fluid mass flow rate and solar radiation will act as indicators for determining the ideal solar panel temperature, PV efficiency, thermal efficiency, and output temperature. Also, the varied changes settings could achieve optimal performance, serving as a valuable reference in experimental approaches and aiding in designing practical research on water-based PVT technology in the field, particularly with rectangular models.

Figure 3 illustrates the output temperature distribution under the highest radiation level of 1000 W/m^2. The maximum temperature recorded in this instance is 74.46 ^{o}C, while the mass flow rate is measured at 0.001 kg/s. In Figure 4, it can be observed that the 0.009 kg/s fluid mass flow rate corresponds to a minimum outlet temperature of 38.42 ^{o}C. Figure 5 illustrates the occurrence of the lowest radiation at 500 W/m^2 intensity, yielding the highest outlet temperature of 51.79 ^{o}C. This thermal response is observed at a 0.001 kg/s fluid mass flow rate. The recorded minimum temperature is 32.82 ^{o}C, corresponding to 0.009 kg/s fluid mass flow rate, as depicted in Figure 6. At a 700 W/m^2 radiation intensity, Figure 7 illustrates that the highest outlet temperature recorded is 60.86 ^{o}C when the fluid mass flow rate is 0.001 kg/s. Conversely, Figure 8 demonstrates that the lowest temperature observed is 34.48 ^{o}C when the fluid mass flow rate is 0.009 kg/s. The simulation results indicate higher solar radiation leads to higher fluid outlet temperatures. Additionally, the results imply an inverse relationship between fluid mass flow rate and collector outlet temperature, suggesting that higher fluid mass flow rates result in lower collector outlet temperatures.

Figure 9 presents the average thermal efficiency and average outlet temperature for various solar radiation levels and fluid mass flow rate ranging from 0.001 kg/s to 0.009 kg/s. Solar radiation significantly affects collector outlet temperature, with values ranging from 500 W/m^2 to 1000 W/m^2. The average outlet temperature reaches a maximum of 50.53 ^{o}C with a 1000 W/m^2 radiation intensity, while it reaches a minimum of 38.92 ^{o}C with a 500 W/m^2 radiation intensity. The highest average thermal efficiency recorded was 64.30% at a 500 W/m^2 radiation level, while the lowest average thermal efficiency observed was 56.34%. Hence, a decrease in solar radiation will increase the average thermal efficiency; conversely, an increase in solar radiation will reduce the average thermal efficiency.

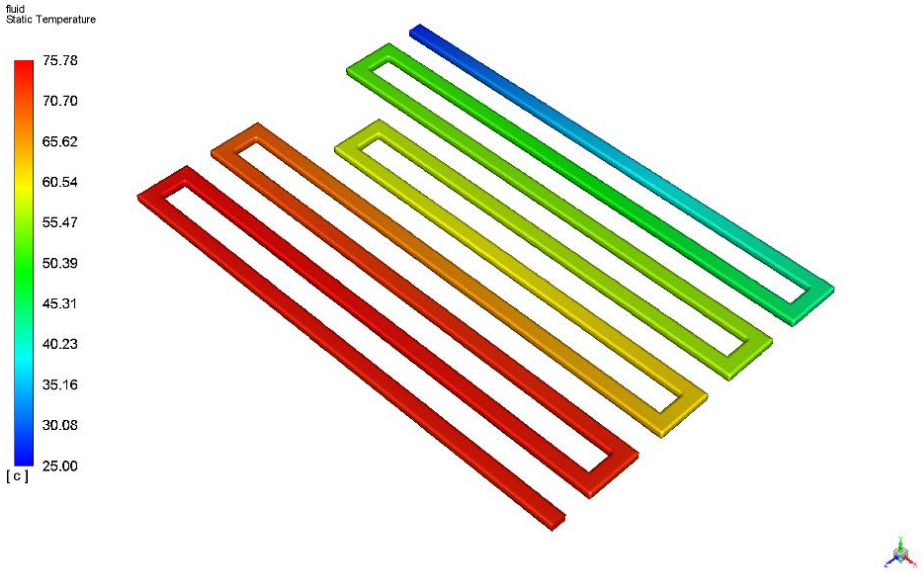

Fig. 3. Highest outlet temperature distribution with 1000 W/m^2 at a 0.001 kg/s fluid mass flow rate

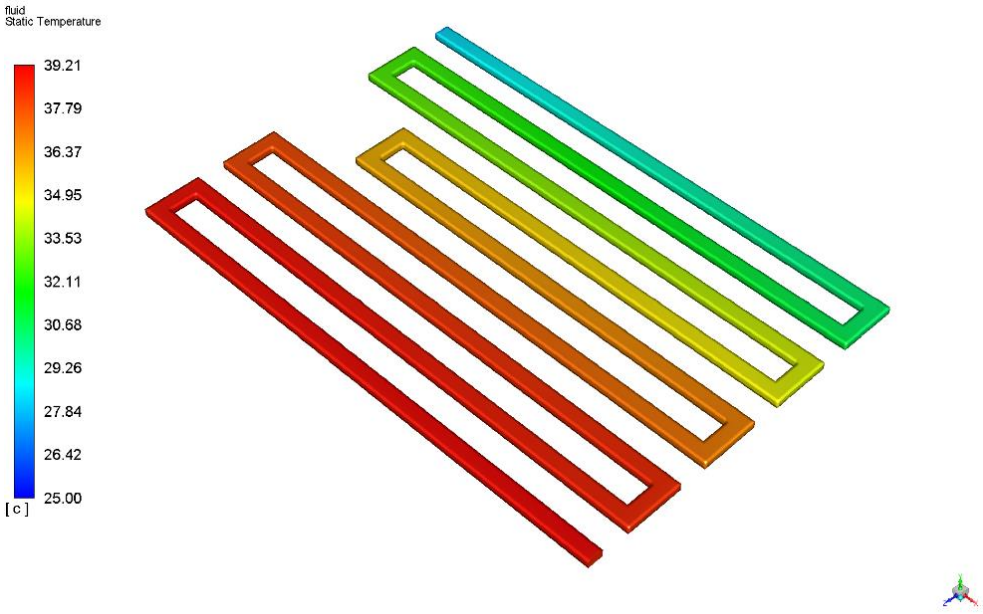

Fig. 4. Lowest outlet temperature distribution at 1000 W/m^2 with a 0.009 kg/s fluid mass flow rate

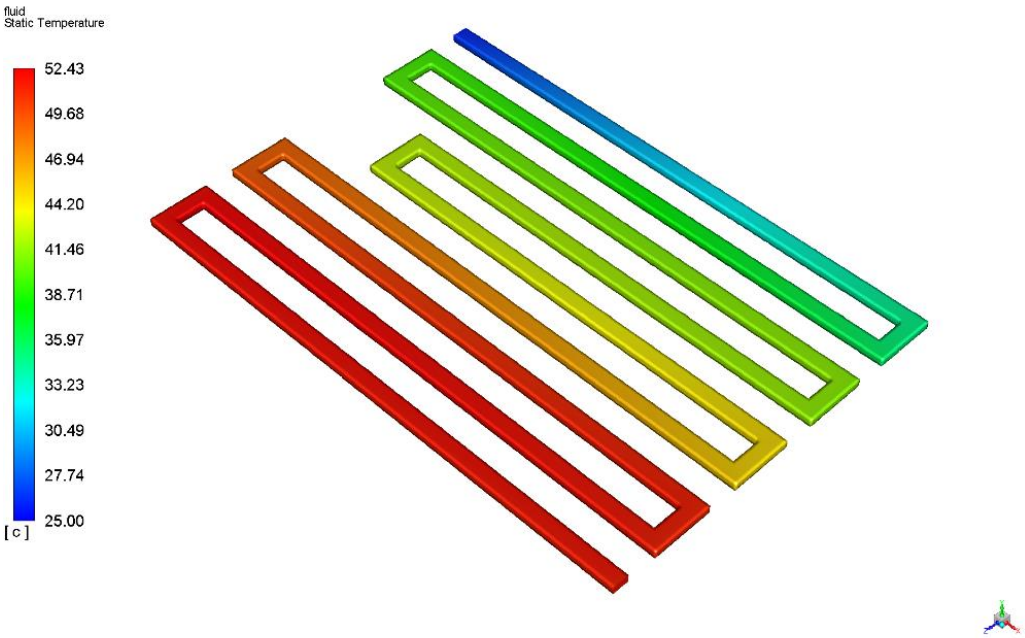

Fig. 5. Highest outlet temperature distribution at 500 W/m^2 with a 0.001 kg/s fluid mass flow rate

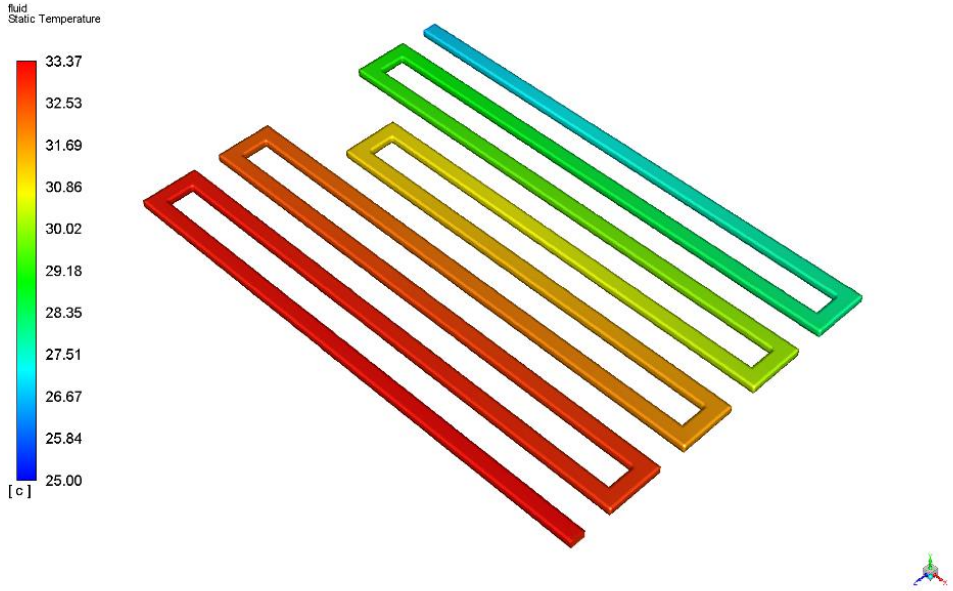

Fig. 6. Lowest outlet temperature distribution at 500 W/m^2 with a 0.009 kg/s fluid mass flow rate

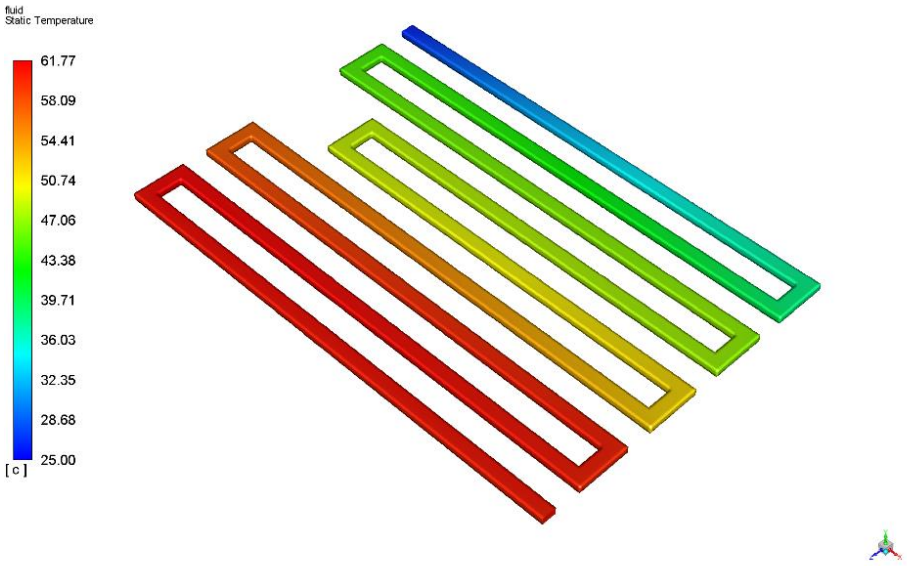

Fig. 7. Highest outlet temperature distribution at 700 W/m^2 with a 0.001 kg/s fluid mass flow rate

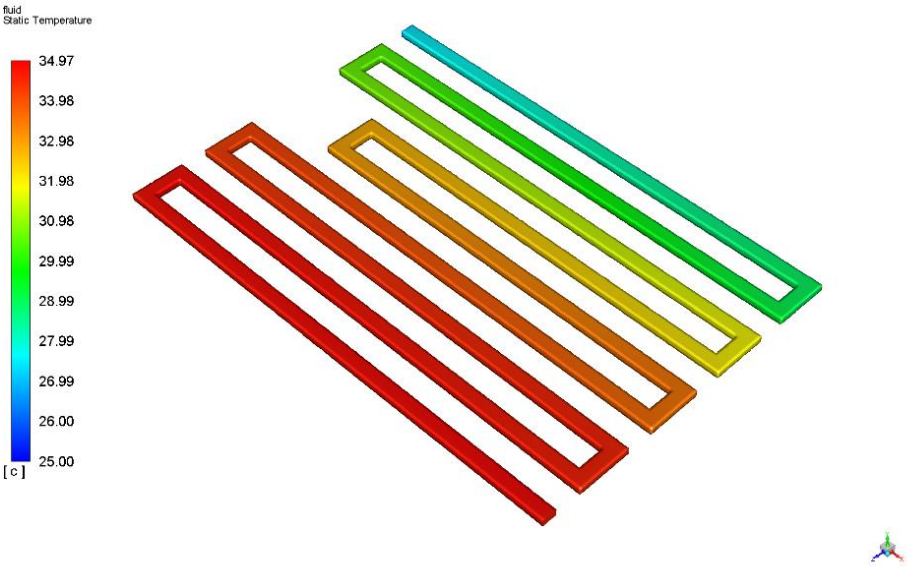

Fig. 8. Lowest outlet temperature distribution at 700 W/m^2 with a 0.009 kg/s fluid mass flow rate

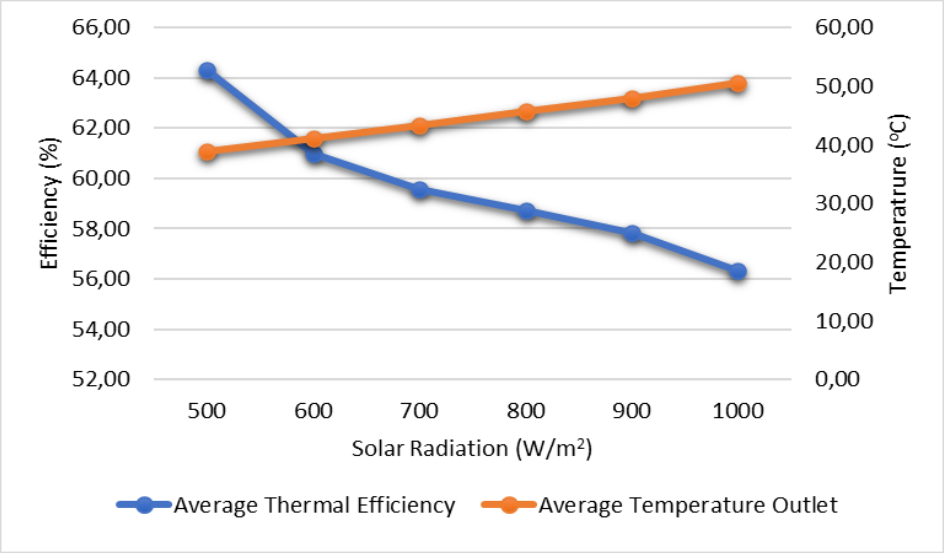

Fig. 9. Average outlet temperature and thermal efficiency of the rectangular channel

Figures 10 to 15 display representative temperature distributions on solar panels at fluid mass flow rates ranging from 0.001 kg/s to 0.009 kg/s while subjecting them to irradiation levels varying from 500 W/m^2 to 1000 W/m^2. The temperature distribution depicted on the solar panel illustrates varying levels of solar radiation and fluid mass flow rate, encompassing high, low, and medium values. Consequently, it covers a wide range of temperature distribution levels. The temperature contour on the solar panel reveals the coldest temperature through the green color, while the red color represents the hottest temperature contour.

The radiation reached its peak at 1000 W/m^2, wherein the maximum temperature of the PV system is recorded as 80.20 ^{o}C with a 0.001 kg/s fluid mass flow rate, as illustrated in Figure 10. Additionally, Figure 11 depicts that the minimum temperature recorded is 48.79 ^{o}C, observed at a 0.009 kg/s fluid mass flow rate. At the 500 W/m^2 minimum radiation level, the maximum temperature of the PV system reaches 54.56 ^{o}C. This temperature is achieved when the fluid mass flow rate is 0.001 kg/s, as seen in Figure 12. Conversely, the minimum temperature recorded is 38.07 ^{o}C, as illustrated in Figure 13. At a 700 W/m^2 medium-level intensity, the highest temperature of the PV module reached 64.81 ^{o}C, as shown in Figure 14, while Figure 15 indicates that the minimum temperature recorded is 41.89 ^{o}C.

Figure 16 exhibits the mean PV temperature and mean PV efficiency for different fluid mass flow rates and solar radiation levels, ranging from 0.001 kg/s to 0.009 kg/s. Solar radiation significantly impacts the PV system's temperature, with values ranging from 500 W/m^2 to 1000 W/m^2. The average PV temperature reaches a peak of 59.08 ^{o}C under 1000 W/m^2 radiation, while it drops to a minimum of 43.25 ^{o}C under 500 W/m^2 radiation. The average PV efficiency ranges from 11.92% at 500 W/m^2 radiation to 11.01%. Hence, a decrease in solar radiation will result in an increase in the average PV efficiency. Conversely, an increase in solar radiation will lead to a reduction in average PV efficiency. Compared to this simulation approach, Rosli *et al.,* [17] reported that the PV efficiency could reach 11.67% with serpentine and spiral absorber designs. The radiation levels ranged from 300 W/m^2 to 1000 W/m^2, and the mass flow rate of fluid went from 0.0005 kg/s to 0.005 kg/s as shown in Table 2.

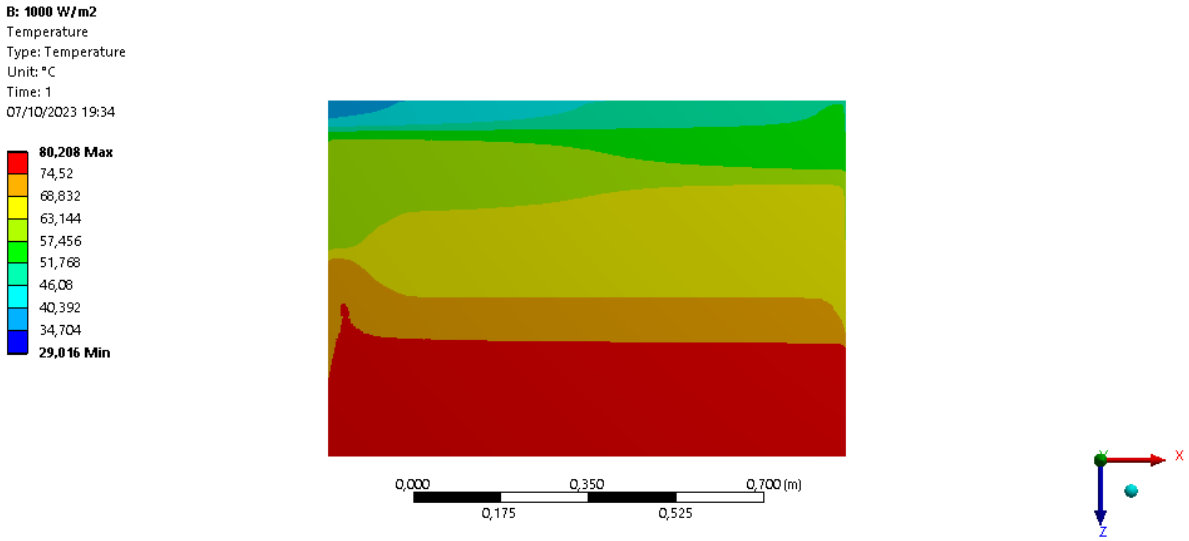

Fig. 10. PV temperature Distribution of 1000 W/m^2 radiation at 0.001 kg/s fluid mass flow rate

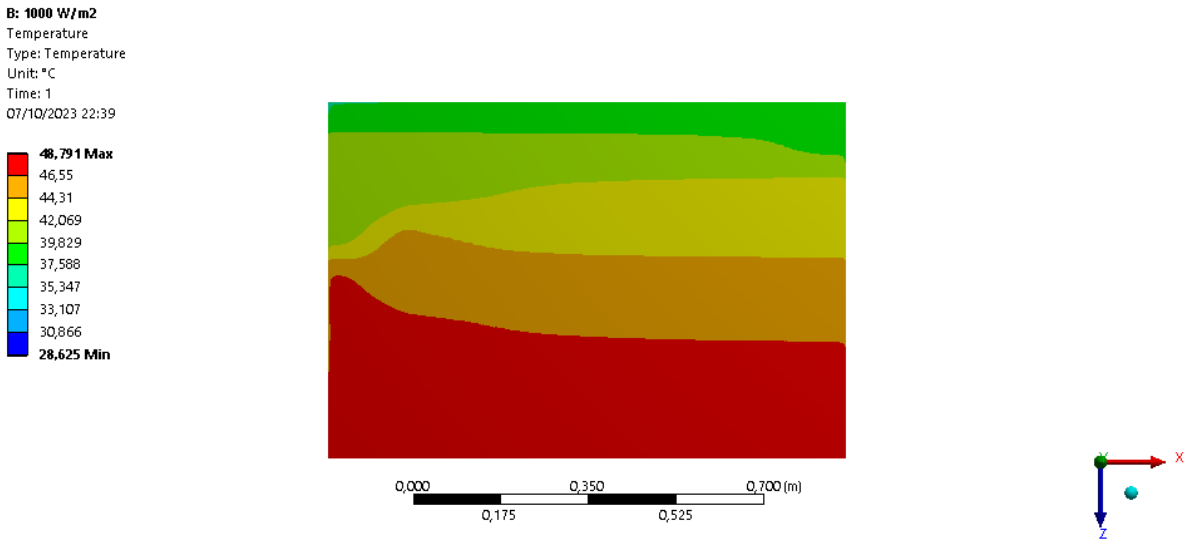

Fig. 11. PV temperature distribution of 1000 W/m^2 radiation at 0.009 kg/s fluid mass flow rate

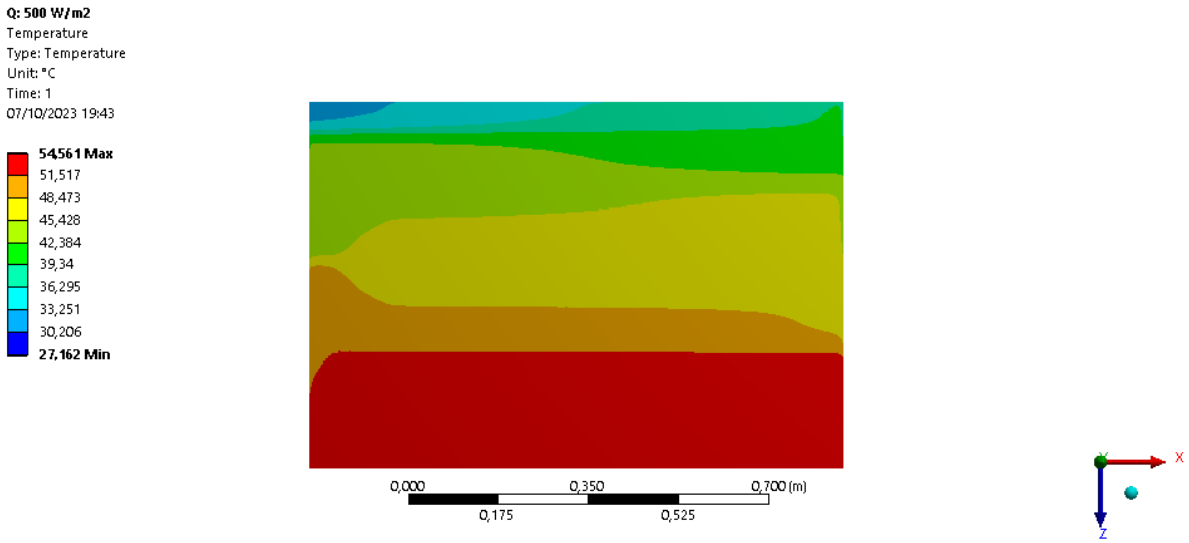

Fig. 12. PV temperature distribution of 500 W/m^2 radiation at 0.001 kg/s fluid mass flow rate

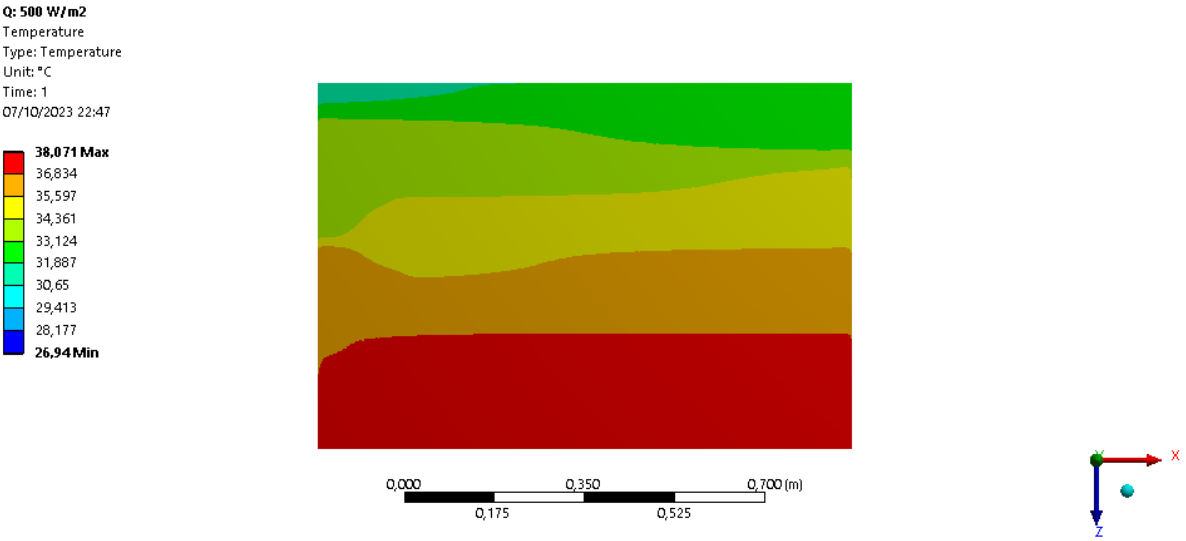

Fig. 13. PV temperature distribution of 500 W/m^2 radiation at 0.009 kg/s fluid mass flow rate

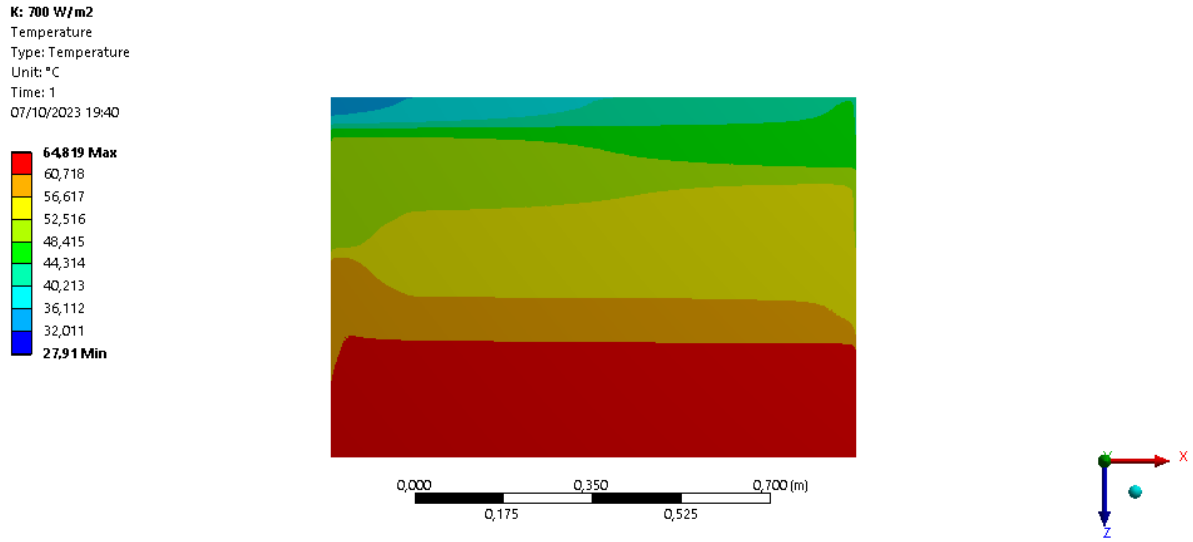

Fig. 14. PV temperature distribution of 700 W/m^2 radiation at 0.001 kg/s fluid mass flow rate

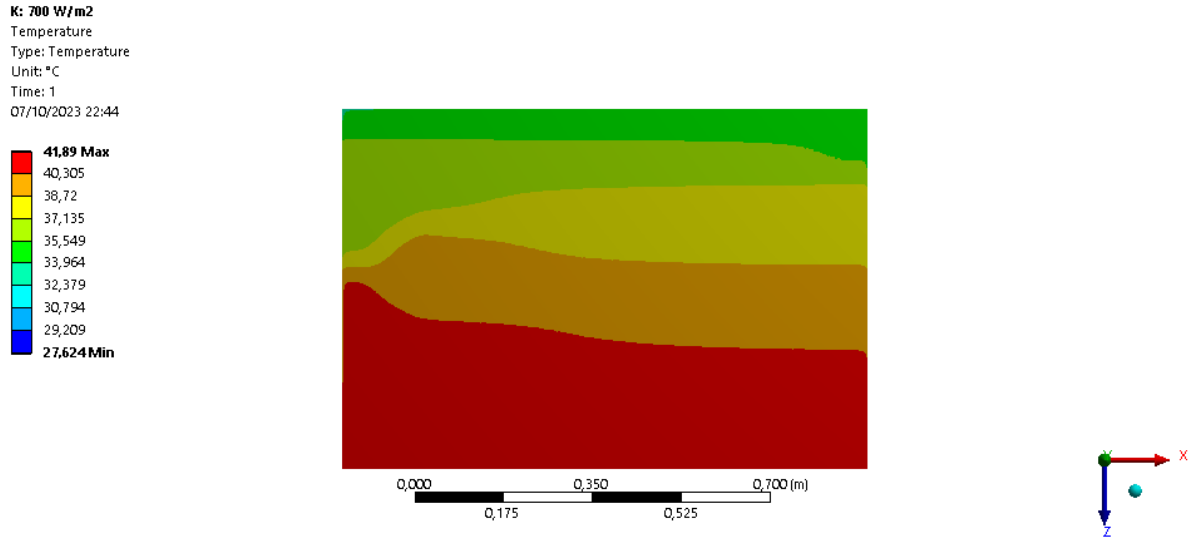

Fig. 15. PV temperature distribution of 700 W/m^2 radiation at 0.009 kg/s fluid mass flow rate

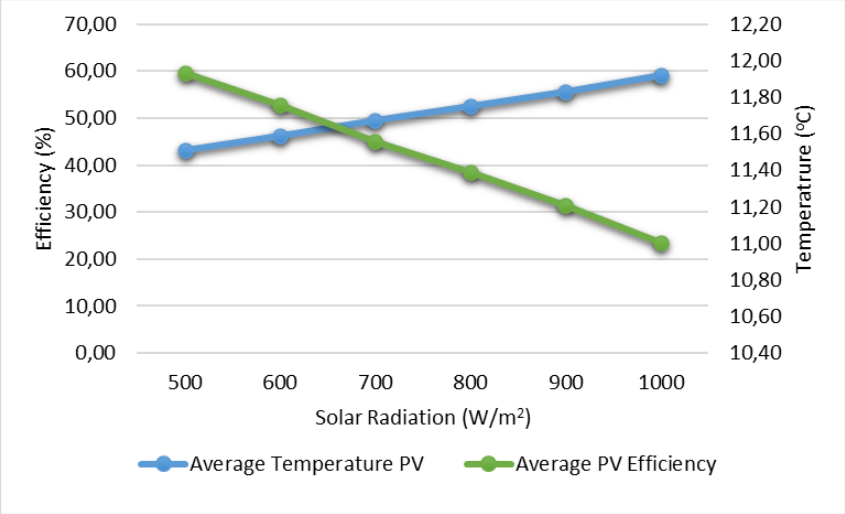

Fig. 16. Average PV temperature and average PV efficiency distribution

The calculation of PVT performance involves the summation of both PV performance and thermal performance. Hence, combining both the thermal and thermal efficiency performance yields an overall photovoltaic thermal efficiency (PVT) performance. Figure 17 illustrates the average efficiency of PVT systems' performance at every level of solar radiation. The range of solar radiation is from 500 W/m^2 to 1000 W/m^2. The rectangular absorber exhibits the maximum average PVT efficiency at a 500 W/m^2 radiation level, with an average efficiency value of 76.23%. Conversely, the lowest average PVT efficiency value is seen at a 1000 W/m^2 radiation level, with an average efficiency value of 69.34%. Therefore, the influence of solar radiation is significant in enhancing the overall performance of a PVT system. In comparison to a rectangular collector-based water fluid with the same water fluid and rectangular absorber, Fudholi *et al.,* [38] reported a PVT efficiency from 63.45% to 76.03%. The solar radiation levels used were 500 W/m^2, 700 W/m^2, and 900 W/m^2. Additionally, the mass flow rate ranged from 0.012 kg/s to 0.0255 kg/s as determined through mathematical modeling and experiment approach, as shown in Table 2.

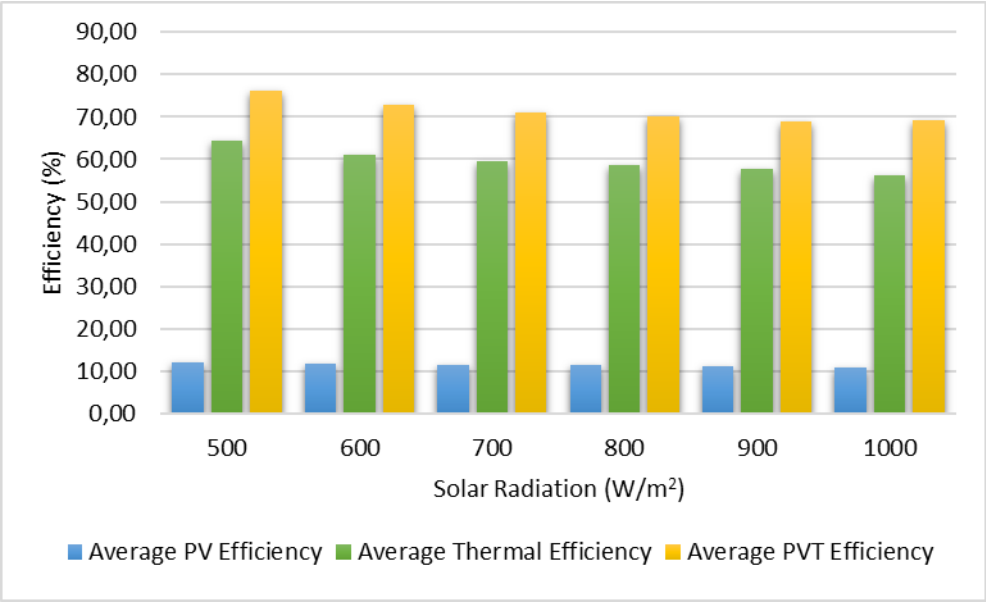

Fig. 17. Average PVT efficiency with different solar radiation

Table 2
Water-based PVT comparison with previous studies

Type of collector	Approach	Finding	Ref.
Roll bond collector PVT by two aluminum	S and E	The yield was alike between S and E.	[39]
Uncover PVT by roll bond	S and E	The E and S results agreed with slight differences.	[40]
Flat plate collector	S and E	The S and E were approved with minor changes.	[41]
Spiral channel	E	PVT efficiency was 68.4%, PV efficiency yielded 13.8%, and thermal efficiency was 54.6%.	[42]
Parabolic dish and high-efficiency collector	M and E	Thermal and electrical efficiency results were similar.	[43]
The harp and serpentine collector model	S	The harp model produces better PVT efficiency performance.	[44]
The serpentine, U-flow, and spiral collector model	S	PV efficiency was 11.67% using the serpentine and spiral model. Thermal efficiencies of serpentine, u-flow, and spiral model were 21.02%, 21.02 and 22.96% respectively. The highest PVT efficiency was 34.63 using the spiral model.	[17]
Rectangular collector model with water, 0.5 wt% TiO2, and 1.0 wt% TiO2 fluid	E and M	The water-based PVT efficiency ranged from 63.45% to 76.03%	[38]

Note: S: simulation, E: experiment, M: Mathematical modeling

4. Conclusions

This study investigates the performance of a water-based rectangular PVT collector system using a CFD methodology. This evaluation encompasses nine different fluid mass flow rate changes and six distinct solar radiation variations. This study examines nine distinct fluid mass flow rate changes, spanning from 0.001 kg/s to 0.009 kg/s, as well as six different solar radiation variations, ranging from 500 W/m^2 to 1000 W/m^2. The temperature distribution of the rectangular channel model and the temperature of the solar panel are both depicted in the study. Based on the analysis results, it can be deduced that the lowest outlet temperature of the rectangular collector is observed when the fluid mass flow rate is 0.009 kg/s and the radiation is 500 W/m^2. On the other hand, the maximum outlet temperature at 1000 W/m^2 radiation intensity with 0.001 kg/s fluid mass flow rate. The maximum thermal efficiency is achieved at a 0.009 kg/s fluid mass flow rate, precisely at a 500 W/m^2 radiation variant. In general, a decrease in outlet temperature leads to an increase in thermal efficiency. The maximum PV efficiency occurs at a 500 W/m^2 radiation level and a 0.009 kg/s fluid mass flow rate. However, the highest average overall efficiency for PVT systems performance is 76.23% at the same radiation level of 500 W/m^2.

References

[1] Siavashi, Majid, Mehdi Vahabzadeh Bozorg, and Mohammad Hesam Toosi. "A numerical analysis of the effects of nanofluid and porous media utilization on the performance of parabolic trough solar collectors." *Sustainable Energy Technologies and Assessments* 45 (2021): 101179. https://doi.org/10.1016/j.seta.2021.101179

[2] Asadian, H., A. Mahdavi, T. B. Gorji, and M. Gorji-Bandpy. "Efficiency improvement of non-crystal silicon (amorphous) photovoltaic module in a solar hybrid system with nanofluid." *Experimental Techniques* 46, no. 4 (2022): 633-645. https://doi.org/10.1007/s40799-021-00498-6

[3] Khelifa, A., K. Touafek, H. Ben Moussa, I. Tabet, and H. Haloui. "Analysis of a hybrid solar collector photovoltaic thermal (PVT)." Energy Procedia 74 (2015): 835-843. https://doi.org/10.1016/j.egypro.2015.07.819

[4] Rosli, M. A. M., S. Mat, K. Sopian, E. Salleh, and M. K. A. Sharif. "Experimental development to determine time constant for polymer collector." *ARPN Journal of Engineering and Applied Sciences* 13 (2006): 1523-1527.

[5] Abdullah, Ahmed L., Suhaimi Misha, Noreffendy Tamaldin, M. A. M. Rosli, and F. A. Sachit. "Photovoltaic thermal/solar (PVT) collector (PVT) system based on fluid absorber design: A review." *Journal of Advanced Research in Fluid Mechanics and Thermal Sciences* 48, no. 2 (2018): 196-208.
[6] Omri, Mohamed, Fatih Selimefendigil, Hichem T. Smaoui, and Lioua Kolsi. "Cooling system design for photovoltaic thermal management by using multiple porous deflectors and nanofluid." *Case Studies in Thermal Engineering* 39 (2022): 102405. https://doi.org/10.1016/j.csite.2022.102405
[7] Salman, Abdul Hakeem A., Kifah H. Hilal, and Safaa A. Ghadhban. "Enhancing performance of PV module using water flow through porous media." *Case Studies in Thermal Engineering* 34 (2022): 102000. https://doi.org/10.1016/j.csite.2022.102000
[8] Masalha, I., S. U. Masuri, O. O. Badran, M. K. A. M. Ariffin, AR Abu Talib, and F. Alfaqs. "Outdoor experimental and numerical simulation of photovoltaic cooling using porous media." *Case Studies in Thermal Engineering* 42 (2023): 102748. https://doi.org/10.1016/j.csite.2023.102748
[9] Kim, Jin-Hee, and Jun-Tae Kim. "Comparison of electrical and thermal performances of glazed and unglazed PVT collectors." *International Journal of Photoenergy* 2012 (2012). https://doi.org/10.1155/2012/957847
[10] Rosli, M. A. M., S. Mat, H. Ruslan, K. Sopian, and Hang Tuah Jaya. "Parametric study on water based photovoltaic thermal collector." In *7th international conference on renewable energy sources (RES'13)*, pp. 135-140. 2013.
[11] Ji, Jie, Jian-Ping Lu, Tin-Tai Chow, Wei He, and Gang Pei. "A sensitivity study of a hybrid photovoltaic/thermal water-heating system with natural circulation." *Applied Energy* 84, no. 2 (2007): 222-237. https://doi.org/10.1016/j.apenergy.2006.04.009
[12] Senthil Kumar, R., N. Puja Priyadharshini, and Elumalai Natarajan. "Experimental and computational fluid dynamics (CFD) study of glazed three dimensional PV/T Solar panel with air cooling." *Applied Mechanics and Materials* 787 (2015): 102-106. https://doi.org/10.4028/www.scientific.net/AMM.787.102
[13] Khan, Firoz, S. N. Singh, and M. Husain. "Effect of illumination intensity on cell parameters of a silicon solar cell." *Solar energy materials and solar cells* 94, no. 9 (2010): 1473-1476. https://doi.org/10.1016/j.solmat.2010.03.018
[14] Sardouei, Masoud Mohammadi, Hamid Mortezapour, and K. A. Z. E. M. JAFARI NAEIMI. "Temperature distribution and efficiency assessment of different PVT water collector designs." *Sādhanā* 43 (2018): 1-13. https://doi.org/10.1007/s12046-018-0826-x
[15] Yu, Ji-Suk, Jin-Hee Kim, and Jun-Tae Kim. "Effect of triangular baffle arrangement on heat transfer enhancement of air-type PVT collector." *Sustainability* 12, no. 18 (2020): 7469. https://doi.org/10.3390/SU12187469
[16] Misha, Simulation, Amira Lateef Abdullah, N. Tamaldin, M. A. M. Rosli, and F. A. Sachit. "Simulation CFD and experimental investigation of PVT water system under natural Malaysian weather conditions." *Energy Reports* 6 (2020): 28-44. https://doi.org/10.1016/j.egyr.2019.11.162
[17] Ping, Yap Joon, Mohd Afzanizam Mohd Rosli, Suhaimi Misha, Mohd Zaid Akop, Kamaruzzaman Sopian, Sohif Mat, Ali Najah Al-Shamani, and Muhammad Asraf Saruni. "Simulation study of computational fluid dynamics on photovoltaic thermal water collector with different designs of absorber tube." *Journal of Advanced Research in Fluid Mechanics and Thermal Sciences* 52, no. 1 (2018): 12-22.
[18] Herrando, María, Alba Ramos, Ignacio Zabalza, and Christos N. Markides. "A comprehensive assessment of alternative absorber-exchanger designs for hybrid PVT-water collectors." *Applied energy* 235 (2019): 1583-1602. https://doi.org/10.1016/j.apenergy.2018.11.024
[19] Arifin, Zainal, Singgih Dwi Prasetyo, Aditya Rio Prabowo, Dominicus Danardono Dwi Prija Tjahjana, and Rendy Adhi Rachmanto. "Effect of thermal collector configuration on the photovoltaic heat transfer performance with 3D CFD modeling." *Open Engineering* 11, no. 1 (2021): 1076-1085. https://doi.org/10.1515/eng-2021-0107
[20] kumar Goel, Abhishek, S. N. Singh, and B. N. Prasad. "Experimental investigation of thermo-hydraulic efficiency and performance characteristics of an impinging jet-finned type solar air heater." *Sustainable Energy Technologies and Assessments* 52 (2022): 102165. https://doi.org/10.1016/j.seta.2022.102165
[21] Singh, Satyender. "Experimental and numerical investigations of a single and double pass porous serpentine wavy wiremesh packed bed solar air heater." *Renewable Energy* 145 (2020): 1361-1387. https://doi.org/10.1016/j.renene.2019.06.137
[22] Eisapour, Amir Hossein, M. Eisapour, M. J. Hosseini, A. H. Shafaghat, P. Talebizadeh Sardari, and A. A. Ranjbar. "Toward a highly efficient photovoltaic thermal module: Energy and exergy analysis." *Renewable Energy* 169 (2021): 1351-1372. https://doi.org/10.1016/j.renene.2021.01.110
[23] Eisapour, M., Amir Hossein Eisapour, M. J. Hosseini, and P. Talebizadehsardari. "Exergy and energy analysis of wavy tubes photovoltaic-thermal systems using microencapsulated PCM nano-slurry coolant fluid." *Applied Energy* 266 (2020): 114849. https://doi.org/10.1016/j.apenergy.2020.114849

[24] Ma, Tao, Meng Li, and Arash Kazemian. "Photovoltaic thermal module and solar thermal collector connected in series to produce electricity and high-grade heat simultaneously." *Applied Energy* 261 (2020): 114380. https://doi.org/10.1016/j.apenergy.2019.114380
[25] Salari, Ali, Arash Kazemian, Tao Ma, Ali Hakkaki-Fard, and Jinqing Peng. "Nanofluid based photovoltaic thermal systems integrated with phase change materials: Numerical simulation and thermodynamic analysis." *Energy Conversion and Management* 205 (2020): 112384. https://doi.org/10.1016/j.enconman.2019.112384
[26] Kolahan, Arman, Seyed Reza Maadi, Arash Kazemian, Corrado Schenone, and Tao Ma. "Semi-3D transient simulation of a nanofluid-base photovoltaic thermal system integrated with a thermoelectric generator." *Energy Conversion and Management* 220 (2020): 113073. https://doi.org/10.1016/j.enconman.2020.113073
[27] Kazemian, Arash, Ali Parcheforosh, Ali Salari, and Tao Ma. "Optimization of a novel photovoltaic thermal module in series with a solar collector using Taguchi based grey relational analysis." *Solar Energy* 215 (2021): 492-507. https://doi.org/10.1016/j.solener.2021.01.006
[28] Baranwal, Naimish Kumar, and Mukesh Kumar Singhal. "Modeling and simulation of a spiral type hybrid photovoltaic thermal (PV/T) water collector using ANSYS." In *Advances in Clean Energy Technologies: Select Proceedings of ICET 2020*, pp. 127-139. Springer Singapore, 2021. https://doi.org/10.1007/978-981-16-0235-1_10
[29] Popovici, Cătălin George, Sebastian Valeriu Hudişteanu, Theodor Dorin Mateescu, and Nelu-Cristian Chereches. "Efficiency improvement of photovoltaic panels by using air cooled heat sinks." *Energy procedia* 85 (2016): 425-432. https://doi.org/10.1016/j.egypro.2015.12.223
[30] Baranwal, Naimish Kumar, and Mukesh Kumar Singhal. "Modeling and simulation of a spiral type hybrid photovoltaic thermal (PV/T) water collector using ANSYS." In *Advances in Clean Energy Technologies: Select Proceedings of ICET 2020*, pp. 127-139. Springer Singapore, 2021. https://doi.org/10.1007/978-981-16-0235-1_10
[31] Khelifa, A., K. Touafek, H. Ben Moussa, and I. Tabet. "Modeling and detailed study of hybrid photovoltaic thermal (PV/T) solar collector." *Solar Energy* 135 (2016): 169-176. https://doi.org/10.1016/j.solener.2016.05.048
[32] Fudholi, Ahmad, Kamaruzzaman Sopian, Mohd Hafidz Ruslan, and Mohd Yusof Othman. "Performance and cost benefits analysis of double-pass solar collector with and without fins." *Energy conversion and management* 76 (2013): 8-19. https://doi.org/10.1016/j.enconman.2013.07.015
[33] Jaaz, Ahed Hameed, Kamaruzzaman Sopian, and Tayser Sumer Gaaz. "Study of the electrical and thermal performances of photovoltaic thermal collector-compound parabolic concentrated." *Results in Physics* 9 (2018): 500-510. https://doi.org/10.1016/j.rinp.2018.03.004
[34] Matheswaran, M. M., T. V. Arjunan, and D. Somasundaram. "Analytical investigation of solar air heater with jet impingement using energy and exergy analysis." *Solar Energy* 161 (2018): 25-37. https://doi.org/10.1016/j.solener.2017.12.036
[35] Abd Elbar, Ayman Refat, and Hamdy Hassan. "Energy, exergy and environmental assessment of solar still with solar panel enhanced by porous material and saline water preheating." *Journal of Cleaner Production* 277 (2020): 124175. https://doi.org/10.1016/j.jclepro.2020.124175
[36] Ewe, Win Eng, Ahmad Fudholi, Kamaruzzaman Sopian, Refat Moshery, Nilofar Asim, Wahidin Nuriana, and Adnan Ibrahim. "Thermo-electro-hydraulic analysis of jet impingement bifacial photovoltaic thermal (JIBPVT) solar air collector." *Energy* 254 (2022): 124366. https://doi.org/10.1016/j.energy.2022.124366
[37] Nazri, Nurul Syakirah, Ahmad Fudholi, Bardia Bakhtyar, Chan Hoy Yen, Adnan Ibrahim, Mohd Hafidz Ruslan, Sohif Mat, and Kamaruzzaman Sopian. "Energy economic analysis of photovoltaic–thermal-thermoelectric (PVT-TE) air collectors." *Renewable and Sustainable Energy Reviews* 92 (2018): 187-197. https://doi.org/10.1016/j.rser.2018.04.061
[38] Fudholi, Ahmad, Nur Farhana Mohd Razali, Mohammad H. Yazdi, Adnan Ibrahim, Mohd Hafidz Ruslan, Mohd Yusof Othman, and Kamaruzzaman Sopian. "TiO2/water-based photovoltaic thermal (PVT) collector: Novel theoretical approach." *Energy* 183 (2019): 305-314. https://doi.org/10.1016/j.energy.2019.06.143
[39] Mishra, R. K., and G. N. Tiwari. "Energy and exergy analysis of hybrid photovoltaic thermal water collector for constant collection temperature mode." *Solar energy* 90 (2013): 58-67. https://doi.org/10.1016/j.solener.2012.12.022
[40] Khelifa, A., K. Touafek, H. Ben Moussa, I. Tabet, and H. Haloui. "Analysis of a hybrid solar collector photovoltaic thermal (PVT)." *Energy Procedia* 74 (2015): 835-843. https://doi.org/10.1016/j.egypro.2015.07.819
[41] Kadhim, Ali Najah, MOHAMMAD H. Yazdi, AZHER M. Abed, M. H. Ruslan, and K. Sopian. "Study on the performance of photovoltaic thermal collector (PV/T) with rectangular tube absorber design." *Computer Applications in Environmental Sciences and Renewable Energy* (2014).
[42] Hussain, F., M. Y. H. Othman, Kamaruzzaman Sopian, Baharudin Yatim, H. Ruslan, and H. Othman. "Design development and performance evaluation of photovoltaic/thermal (PV/T) air base solar collector." *Renewable and Sustainable Energy Reviews* 25 (2013): 431-441. https://doi.org/10.1016/j.rser.2013.04.014

[43] Aste, Niccolò, Claudio Del Pero, Fabrizio Leonforte, and Massimiliano Manfren. "Performance monitoring and modeling of an uncovered photovoltaic-thermal (PVT) water collector." *Solar Energy* 135 (2016): 551-568. https://doi.org/10.1016/j.solener.2016.06.029

[44] Aste, Niccolò, Fabrizio Leonforte, and Claudio Del Pero. "Design, modeling and performance monitoring of a photovoltaic–thermal (PVT) water collector." *Solar Energy* 112 (2015): 85-99. https://doi.org/10.1016/j.solener.2014.11.025